Microcavity confinement based on an anomalous zero group-velocity waveguide mode

Mihai Ibanescu, Steven G. Johnson, David Roundy, Yoel Fink, and J. D. Joannopoulos

Center for Materials Science and Engineering, Massachusetts Institute of Technology, Cambridge, Massachusetts 02139

Received October 1, 2004

We propose and demonstrate a mechanism for small-modal-volume high-Q cavities based on an anomalous uniform waveguide mode that has zero group velocity at a nonzero wave vector. In a short piece of a uniform waveguide with a specially designed cross section, light is confined longitudinally by small group-velocity propagation and transversely by a reflective cladding. The quality factor Q is greatly enhanced by the small group velocity for a set of cavity lengths that are separated by approximately π/k_0, where k_0 is the longitudinal wave vector for which the group velocity is zero. © 2005 Optical Society of America

OCIS codes: 230.5750, 230.7370.

Optical microcavities with small modal volumes and large quality factors are required in a wide range of applications and studies, such as low-threshold lasers, small optical filters, nonlinear optics, and strong-coupling cavity quantum electrodynamics.[1–6] Cavities with a modal volume V of the order of λ^3 tend to have quality factors Q that are limited by radiation loss. Several mechanisms have been used to improve Q without sacrificing the small modal volume: the use of a complete photonic bandgap in a three-dimensional photonic crystal,[7] perfect mode matching in a cylindrical Bragg resonator,[8] Fourier-space analysis of the field distribution in a photonic crystal slab cavity,[9,10] and multipole cancellation in a photonic crystal slab cavity.[11] Here we introduce a fundamentally different mechanism based on small group-velocity propagation of light in a short piece of a uniform waveguide. The small group velocity results in a large Q in two ways: (i) it increases the round-trip travel time inside the cavity, and (ii) it decreases the fraction of power lost at each reflection from the boundaries (even though the structure includes no conventional high-quality mirrors in the axial direction). A critical requirement is that the zero group velocity be associated with a nonzero wave vector so that the Fabry–Perot resonance condition can be met.

The design of the cavity is based on the possibility of uniform waveguides to support modes with zero group velocity at a nonzero longitudinal wave vector. It was shown recently[12] that such modes can be created in waveguides with an arbitrary cross section, provided that the waveguides have a reflective cladding, such as a metal layer, a dielectric mirror, or a two-dimensional photonic crystal cladding. To demonstrate the novel high-Q mechanism we first consider a simple cavity based on an idealized dielectric-loaded metal waveguide. Then we show how the same mechanism can be exploited in a realistic structure by designing an all-dielectric high-Q cavity.

Let us first consider the dielectric-loaded metal waveguide whose cross section is shown as an inset in Fig. 1. Inside a metal cylinder of inner radius a, we have a dielectric rod of radius $0.65a$ and a refractive index $n_1 = 3.50$ surrounded by a region with a low refractive index $n_0 = 1$. Dispersion relations $\omega(k)$ are shown for the lowest two guided modes with angular momentum unity: HE_{11} and EH_{11}. Strong repulsion between the two modes is visible for wave vectors $k > 0$, because of the removal of a TE/TM symmetry that exists only at $k = 0$.[12] As a result, the lower mode acquires an anomalous dispersion relation that includes a region of backward-wave propagation[13] for k less than $k_0 = 0.146\ (2\pi/a)$, as well as a point of zero group velocity at wave vector k_0 and angular frequency $\omega_0 = 0.1656\ (2\pi c/a)$. This special point of the dispersion relation introduces a longitudinal length scale $\Lambda = 2\pi/k_0 = 6.85a$ in a waveguide that is otherwise uniform. Now, imagine an optical cavity that is simply a piece of length L of the waveguide described above, surrounded by vacuum, as shown in Fig. 2(a). The resonant modes of the cavity obey the condition that the round-trip accumulated phase

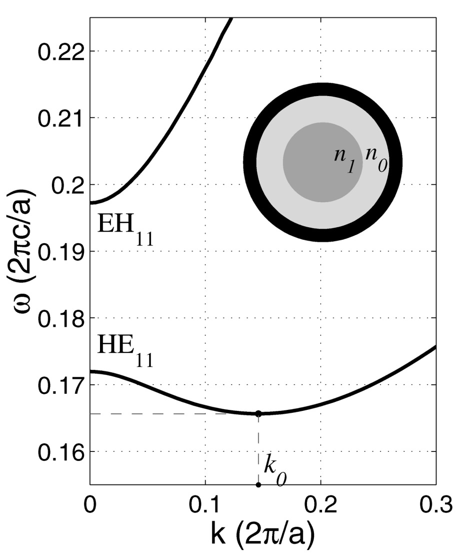

Fig. 1. Band structure of the axially uniform dielectric-loaded metal waveguide (inset) showing the lowest two modes. The lower mode is anomalous with a nontrivial point of zero group velocity at $k_0 = 0.146\ (2\pi/a)$, $\omega_0 = 0.1656\ (2\pi c/a)$.

0146-9592/05/050552-03$15.00/0

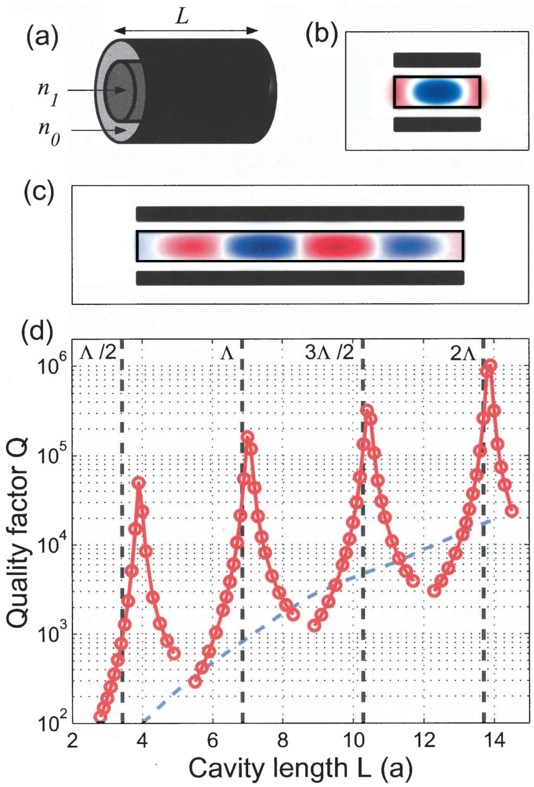

Fig. 2. (a) A piece of the waveguide of length L in Fig. 1 can form a high-Q cavity. (b) Resonant mode in a cavity of length $L = 3.9a$. In an axial cross section we show the electric field component perpendicular to the plane, with the red and blue regions corresponding to positive and negative values, respectively. The metal cladding is shown in black. Note that the finite-difference time-domain computational cell is actually larger than the rectangular box shown here. (c) Resonant mode for $L = 13.9a$. (d) Q is plotted as a function of cavity length L. The red circles are the results of finite-difference time-domain simulations, and the dashed vertical lines correspond to multiples of $\Lambda/2$. Also shown as a blue dashed line is the $Q(L)$ curve for a cavity based on a modified waveguide that does not have $v_g = 0$ at $k \neq 0$.

$2kL + 2\Delta\phi$ is a multiple of 2π, where $\Delta\phi$ is the phase shift associated with reflection from the boundary and is roughly independent of L. For lengths L separated by $\Lambda/2 = \pi/k_0$, the resonance condition is met for wave vectors close to k_0, and therefore Q of the resonant mode should be enhanced by the low group velocity. Thus we expect $Q(L)$ to have a periodic enhancement, with periodicity $\Lambda/2$.

We analyze the resonant modes of the cavity with finite-difference time-domain simulations, using a resolution of 20 grid points per a and perfectly matched absorbing boundary layers.[14] To speed up the calculations we discretize the structure over a cylindrical grid and impose an angular field dependence of the form $\exp(i\varphi)$, thus selecting only modes with angular momentum unity and reducing a full three-dimensional problem to a two-dimensional simulation. We excite the resonant mode of interest with a Gaussian pulse and then monitor the radiative decay of the field. The frequencies and quality factors of resonant modes are extracted with a filter-diagonalization method that decomposes a time series into a sum of decaying sinusoids.[15] In Fig. 2(b) we show the high-Q resonant mode found in a cavity of length $L = 3.9a$. The mode has angular frequency $0.1711\ (2\pi c/a)$, quality factor $Q \simeq 49{,}000$, and modal volume $0.6\ (\lambda/n_1)^3$. Similarly, for $L = 13.9a$, Fig. 2(c) shows a mode with $\omega = 0.1622\ (2\pi c/a)$, $Q \simeq 1.0 \times 10^6$, and modal volume $1.4\ (\lambda/n_1)^3$. From the two field patterns, we infer that these two resonant modes are based on the same mode of the uniform waveguide, the difference being the number of half-wavelengths that fit inside the cavity: one and four, respectively. Figure 2(d) shows on a semi-logarithmic scale how Q varies with the length of cavity L. We plot the $Q(L)$ curve as four disconnected sections because the mode with the highest Q value changes from having one half-wavelength in the cavity to having two, three, or four half-wavelengths. The immediate qualitative conclusion from Fig. 2(d) is that there is indeed a longitudinal length scale associated with the waveguide, this being reflected in the periodic behavior of $Q(L)$. Moreover, the cavity lengths for which $Q(L)$ peaks are separated by almost exactly $\Lambda/2$. Actually, the peak lengths themselves lie very close to the multiples of $\Lambda/2$ shown as dashed vertical lines in the figure, which is consistent with a reflection phase shift $\Delta\phi$ being close to π. As L becomes larger, the frequency of the resonant mode converges quadratically to ω_0, the frequency of zero group velocity in the uniform waveguide. All the results presented above support our conclusion that the high-Q resonant mode indeed has its origin in the zero group-velocity mode of the waveguide and that the longitudinal length scale Λ of the waveguide is critical for determining the cavity lengths for which Q is maximum. For comparison, the dashed blue curve in Fig. 2 is the $Q(L)$ curve for a waveguide in which the radius of the central rod has been reduced to $0.40a$. This waveguide still has a flattened dispersion relation for the HE_{11} mode but does not have a mode with $v_g = 0$ at $k \neq 0$, and thus its $Q(L)$ curve does not possess any periodicity.

To verify that the results presented above are general and not just a coincidence for a particular waveguide structure, we repeat the $Q(L)$ calculations for other values of refractive index n_1 and summarize the results in Table 1. For each n_1 we list the wave vector k_0 at which the waveguide mode has zero group velocity and cavity length L_4 that corresponds to the fourth peak of curve $Q(L)$. Our simple model based on the round-trip phase shift predicts that $2k_0L_4$ should be in the neighborhood of 8π. Indeed, we find that $2k_0L_4$ is always close to the predicted value. Moreover, a change in k_0 of $\sim$10% from $n_1 = 3.50$ to $n_1 = 3.90$ results in a change of only 1% for phase shift $2k_0L_4$.

Table 1. Conservation of Round-Trip Phase Shift

n_1	$k_0\ (2\pi/a)$	$L_4\ (a)$	$2k_0L_4$
3.50	0.146	13.9	8.08π
3.70	0.161	12.4	8.02π
3.90	0.172	11.6	7.98π

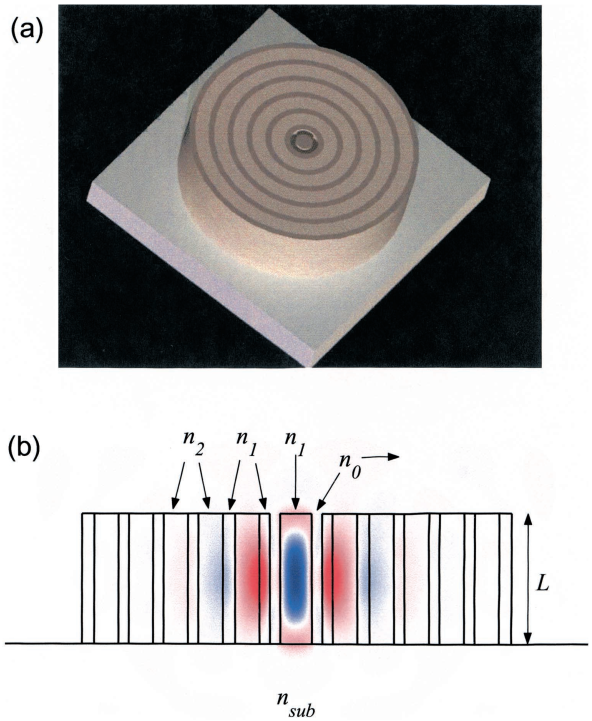

Fig. 3. (a) Cylindrical all-dielectric cavity. (b) Axial cross section of the cavity structure: on top of a substrate with refractive index n_{sub}, we have a central rod with index n_1 followed by a region with index n_0 and surrounded by a Bragg mirror that confines light to the core region. The electric field component perpendicular to the plane is shown in a color plot.

Having shown that zero group-velocity modes can lead to high-Q resonances, we apply this mechanism to the design of an all-dielectric high-Q cavity. As shown in Ref. 12, modes with $v_g = 0$ at a nonzero wave vector can be found in dielectric waveguides such as cylindrical Bragg fibers and photonic crystal fibers. Here we choose the former waveguide type as an example and design a cavity geometry, shown in Fig. 3, that should be manufacturable by lithographic methods. The core part is similar to the cavity presented before: a central rod with index $n_1 = 3.50$ (e.g., silicon) and radius $0.60a$, surrounded by a region with refractive index $n_0 = 1$ up to a radius a. The rest of the structure is the Bragg mirror that confines light to the core region. The mirror is made from alternating layers: high-index layers with index n_1 and thickness $d_1 = 0.40a$ and low index layers with $n_2 = 1.45$ (e.g., silica) and $d_2 = 0.95a$. The cavity sits on a substrate with index n_{sub}. We first calculate the modes of a waveguide that has these cross-section parameters and find a bandgap-guided mode with $v_g = 0$ at $k_0 = 0.12\ (2\pi/a)$ and $\omega_0 = 0.182\ (2\pi c/a)$. We expect to create a high-Q resonant mode when the cavity length (or height in this case) is near $\Lambda/2 = \pi/k_0$. Indeed, for $L = 4.8a$ and a symmetric structure with $n_{\text{sub}} = n_0 = 1$, we find a resonant mode with frequency $0.184\ (2\pi c/a)$, $Q = 17{,}000$ and modal volume $1.1\ (\lambda/n_1)^3$. In the core region the field distribution shown in Fig. 3(b) is very similar to that obtained for the analogous metallic cavity. Also, the frequency of the resonant mode is only 1% away from ω_0. Thus we conclude that this high-Q mode is also due to the spatial zero group-velocity point of the dispersion relation. Taking a higher value for the substrate refractive index leads to a decrease in Q because power leaks more easily into a high-refractive-index region. For $n_{\text{sub}} = 1.30$ and $L = 5.00$ the quality factor is reduced by $\sim$50% to $Q = 7500$. Since this reduction factor is approximately the same for longer cavities, larger Q values can be obtained for cavities designed to fit higher-order resonant modes as in Fig. 2(d).

In conclusion, we have described a general mechanism for obtaining high-Q resonant modes starting from uniform waveguide modes with zero group velocity at a nonzero wave vector. We demonstrated the mechanism in a simple metal cavity and showed that the same mechanism can be applied to all-dielectric cavities as well. It is our hope that, by itself or in combination with previously studied mechanisms, this new high-Q mechanism will allow for the design and fabrication of improved optical microcavities.

This work was supported by the Materials Research Science and Engineering Center program of the National Science Foundation under grant DMR-9400334. M. Ibanescu's e-mail address is michel@mit.edu.

References

1. K. J. Vahala, Nature **424,** 839 (2003).
2. O. Painter, R. K. Lee, A. Scherer, A. Yariv, J. D. O'Brien, P. D. Dapkus, and I. Kim, Science **284,** 1819 (1999).
3. M. Soljacic, M. Ibanescu, S. G. Johnson, J. D. Joannopoulos, and Y. Fink, Opt. Lett. **28,** 516 (2003).
4. J. Vuckovic and Y. Yamamoto, Appl. Phys. Lett. **82,** 2374 (2003).
5. D. Ochoa, R. Houdre, M. Ilegems, H. Benisty, T. F. Krauss, and C. J. M. Smith, Phys. Rev. B **61,** 4806 (2000).
6. J. Vuckovic, M. Loncar, H. Mabuchi, and A. Scherer, Phys. Rev. E **65,** 016608 (2000).
7. J. D. Joannopoulos, P. R. Villeneuve, and S. Fan, Nature **386,** 143 (1997).
8. M. R. Watts, S. G. Johnson, H. A. Haus, and J. D. Joannopoulos, Opt. Lett. **27,** 1785 (2002).
9. Y. Akahane, T. Asano, B.-S. Song, and S. Noda, Nature **425,** 944 (2003).
10. K. Srinivasan and O. Painter, Opt. Express **10,** 670 (2002), http://www.opticsexpress.org.
11. S. G. Johnson, S. Fan, A. Mekis, and J. D. Joannopoulos, Appl. Phys. Lett. **78,** 3388 (2001).
12. M. Ibanescu, S. G. Johnson, D. Roundy, C. Luo, Y. Fink, and J. D. Joannopoulos, Phys. Rev. Lett. **92,** 063903 (2004).
13. P. J. B. Clarricoats and R. A. Waldron, J. Electron. Control **8,** 455 (1960).
14. A. Taflove and S. C. Hagness, *Computational Electrodynamics: the Finite-Difference Time-Domain Method*, 2nd ed. (Artech, Norwood, Mass., 2000).
15. V. A. Mandelshtam and H. Taylor, J. Chem. Phys. **107,** 6756 (1997).